Biomedicine & Pharmacotherapy 155 (2022) 113669

Contents lists available at ScienceDirect

Biomedicine & Pharmacotherapy

journal homepage: www.elsevier.com/locate/biopha

PARP1 inhibition by Olaparib reduces the lethality of pancreatic cancer cells and increases their sensitivity to Gemcitabine

Francisco Quiñonero [a,b,c], Cristina Mesas [a,b,c], Jose A. Muñoz-Gámez [a], Cristina Jiménez-Luna [a,b,c], Gloria Perazzoli [a,b,c], Jose Prados [a,b,c,*], Consolación Melguizo [a,b,c,1], Raul Ortiz [a,b,c,1]

[a] Institute of Biopathology and Regenerative Medicine (IBIMER), Center of Biomedical Research (CIBM), University of Granada, Granada 18100, Spain
[b] Department of Anatomy and Embryology, Faculty of Medicine, University of Granada, Granada 18071, Spain
[c] Instituto Biosanitario de Granada (ibs. GRANADA), Granada 18014, Spain

ARTICLE INFO

Keywords:
PARP1
Pancreatic cancer
Olaparib
Gemcitabine
Drug resistance

ABSTRACT

Pancreatic cancer (PC) is one of the tumors with the lowest survival rates due to the poor efficacy of the treatments currently used. Gemcitabine (GMZ), one of the chemotherapeutic agents employed when the tumor is unresectable, frequently fails due to the development of drug resistance. PARP1 is a relevant protein in this phenomenon and appears to be related to cancer progression in several types of tumors, including PC. To determine the relevance of PARP1 in the development and treatment of PC, we used the Panc02 cell line to generate modified PC cells with stably inhibited PARP1 expression (Panc02-L) and used GMZ, Olaparib (OLA) and GMZ+OLA as therapeutic strategies. Viability, radiosensitization, angiogenesis, migration, colony formation, TUNEL, cell cycle, multicellular tumorsphere induction and *in vivo* assays were performed to test the influence of PARP1 inhibition on resistance phenomena and tumor progression. We demonstrated that stable inhibition or pharmacological blockade of PARP1 using OLA-sensitized Panc02 cells against GMZ significantly decreased their IC_{50}, reducing colony formation capacity, cell migration and vessel formation (angiogenesis) in vitro. Furthermore, *in vivo* analyses revealed that Panc02-L-derived (PARP1-inhibited) tumors showed less growth and lethality, and that GMZ+OLA treatment significantly reduced tumor growth. In conclusion, PARP1 inhibition, both alone and in combination with GMZ, enhances the effectiveness of this chemotherapeutic agent and represents a promising strategy for the treatment of PC.

1. Introduction

Pancreatic ductal adenocarcinoma, commonly known as pancreatic cancer (PC), accounted for 2.6 % of all cancers in 2020 [1]. Despite its precise etiology remains unknown, PC showed a higher prevalence in the presence of risk factors such as smoking, alcohol consumption, high cholesterol, physical inactivity, obesity, and hypertension [2]. Due to the absence of symptoms or presence of unspecific symptoms, most patients are diagnosed at advanced stages of the disease, when surgery, the only option to cure PC, is not an effective therapy. Therefore, the 5-year survival rate is very low, and the prognosis is generally poor [3,4]. Specifically, 80–85 % of PC are unresectable at diagnosis. In these cases, palliative chemotherapy, including gemcitabine (GMZ), is the treatment of choice. In addition, of the 15–20 % of patients who have resectable tumours, 75 % of patients have recurrences within 5 years [5]. It is therefore necessary to find a treatment to prevent tumour recurrence after removal. New adjuvant chemotherapy protocols, such as the 5-fluorouracil derivative (S-1), GMZ combined with

Abbreviations: CI, combination index; CSC, cancer stem cell; CSC-L, cancer stem-like cell; GMZ, Gemcitabine; p-γ-H2AX, Histone H2AX phosphorylated; IC, inhibitory concentration; IR, radiotherapy; MTS, multicellular tumor spheroids; OLA, Olaparib; PARP1, Poly [ADP-ribose] polymerase 1; PARPi, PARP inhibitor; PC, pancreatic cancer; P/S, penicillin-streptomycin; preOLA, Olaparib pre-treatment; RT-qPCR, real time quantitative PCR; SRB, Sulforhodamine B; SSRB, single-stranded damage repair; TCA, trichloroacetic acid; Tm, annealing temperatures.

* Corresponding author at: Institute of Biopathology and Regenerative Medicine (IBIMER), Center of Biomedical Research (CIBM), University of Granada, Granada 18100, Spain.
E-mail address: jcprados@ugr.es (J. Prados).
[1] Co-senior author: equal contribution.

https://doi.org/10.1016/j.biopha.2022.113669
Received 1 July 2022; Received in revised form 29 August 2022; Accepted 5 September 2022
Available online 13 September 2022

nab-paclitaxel, and modified FOLFIRINOX regime, have been approved to PC treatment. Nevertheless, drug toxicity and high tumor resistance to chemotherapy limit their efficacy [6,7].

In this context, Poly (ADP-ribose) polymerases 1 and 2 (PARP1 and PARP2), two members of a protein family involved in DNA damage response, have been implicated in PC drug resistance [8,9]. Recently, *in vitro* studies using PC cells show that cytoplasmic expression of PARP1 induced cell death resistance, avoiding apoptosis mediated by TRAIL receptors [10]. Overexpression of *PARP1* has been also described in some types of carcinomas (breast, uterine, ovarian, lung and skin) and lymphomas (non-Hodgkin) [11,12]. Then, inhibition of pathways involved in DNA damage repair to avoid cell apoptosis, has been proposed as a strategy to improve cancer treatment [13]. The effect of PARP1 inhibitors in PC generally depends on the existence of BRCA gene mutations (8 % of PC patients) in the initial tumor [5]. These genes synthesise tumour suppressors responsible for repairing double-stranded DNA damage. When this repair pathway is lacking in conjunction with PARP1 inhibition, a phenomenon called synthetic lethality occurs and the tumour cell dies. Nevertheless, PARP1 inhibitors as Olaparib can exert their effect through other alternative routes such as the inhibition of single-stranded damage repair (SSRB), the PARP trapping or preventing the oncogene transcription so it could be an interesting therapy strategy for BRCA wild type patients [14]. In recent years, several specific PARP1 inhibitors (PARPi) have been developed and some of them have been approved by the US Food and Drug Administration (FDA), including Rucaparib, Niraparib, and Olaparib (OLA). Specifically, OLA has been tested in clinical trials for different cancer types, including breast (NCT02032823, NCT02000622), ovarian (NCT01844986) and pancreatic cancer (NCT02184195) [15].

Interestingly, adjuvant treatment using OLA in patients with BRCA-mutated, HER2-negative breast cancer induced low mortality compared to classical chemotherapy. Furthermore, BRCA-negative pancreatic cancer patients who did not respond to platinum-based therapies, showed some improvement after Olaparib treatment. By contrast, OLA was not effective in ovarian cancer [16,17]. However, this PARPi was able to improve the effect of radiotherapy in ovarian and lung cancer [18,19]. Other PARPi drugs, such as veliparib, a PARP1 and 2 inhibitor, or Talazoparib, are being used in ovarian and breast cancer [20–22]. However, only a small subset of patients appears to respond to this treatment [23].

On the other hand, cancer stem cells (CSCs) exhibit high resistance to chemoradiotherapy through different mechanisms, including overexpression of ABC transporters, detoxifying enzymes and proteins involved in cell death processes [24]. In addition, this cell population is relevant in tumour recurrence after chemotherapeutic treatment and in the development of metastasis [25]. Interestingly, PARP1 overexpression has been detected in breast CSCs, suggesting that this protein plays an important role in resistance against traditional drugs [26] and that its inhibition could induce sensitization of these cells to chemotherapy [27]. Recently, we demonstrated that there is a high expression of *PARP1* in CSCs of pancreatic, liver and colon cancers [28], which suggests that it may be a common resistance mechanism of gastrointestinal tumours. In this context, we hypothesize that the use of PARPi could induce specific damage to CSCs, reducing cancer recurrence and metastasis.

The aim of this work was to determine the effect of PARP1 inhibition in the development of PC, both *in vitro* (using PARP1 positive cells and cells with inhibited PARP1), and *in vivo* (using PC tumours generated in mice), and to determine the effect of combining the inhibition of PARP1 with GMZ to avoid drug resistance. Our results could represent a promising novel strategy to improve the treatment of patients with PC.

2. Methods

2.1. Cell culture

The murine pancreatic adenocarcinoma cell line Panc02 was kindly provided by Dr. Lars Ivo Partecke, University of Greifswald, Germany. Panc02-L cell line was obtained from Panc02 cells after stable transduction as described below. Both pancreatic cancer cell lines were grown in Dulbecco's modified Eagle's medium (DMEM) (Sigma-Aldrich, San Luis, EEUU) supplemented with 10 % fetal bovine serum (FBS) (Thermo Fisher, Waltham, Massachusetts, EEUU) and 1 % penicillin-streptomycin solution (P/S) (Sigma-Aldrich). Cells were maintained in a monolayer culture in a 37 °C and 5 % CO_2 atmosphere.

2.2. Cellular transduction

To carry out lentiviral transduction, lentiviral vectors containing stable expression siRNAs against PARP1 (sc-29437-V, Santa Cruz Biotechnology, Dallas, Texas, EEUU), and control shRNA lentiviral particles were used (sc-108080, Santa Cruz Biotechnology). Panc02 cells were seeded in 6-well plates (Thermo Fisher) in supplemented DMEM medium and incubated overnight. Then, a mixture containing supplemented DMEM and Polybrene (sc-134220, Santa Cruz Biotechnology, Dallas, Texas, EEUU) was prepared at 5 μg/ml and added to the cells 20 min after transduction. Then, control and PARP1 shRNA lentiviral particles were thawed and added to each well, shaking the plate for homogeneous distribution. Cells were incubated overnight and then the medium was changed to supplemented DMEM. For 2–3 weeks, the transduced cells were selected using puromycin dihydrochloride at 2 μg/ml after finding that untransducent cells died when this concentration was used (sc-108071, Santa Cruz Biotechnology), generating the Panc02-L cell line (PARP1 negative).

2.3. Cancer stem-like cells induction

Induction was carried out following previously established protocols [29]. To obtain cancer stem-like cells (CSC-L), Panc02 and Panc02-L cell lines were trypsinized and cultured in a tumor stem cell selection medium with DMEM-F12 medium, hydrocortisone (Sigma-Aldrich, 1 μg/ml), heparin (Sigma-Aldrich, 4 ng/ml), human epithelial growth factor (Sigma-Aldrich, 10 ng/ml) and human fibroblast growth factor (Sigma-Aldrich, 20 ng/ml), ITS-G (Thermo Fisher, 10 μg/ml), B27 vitamin (Thermo Fisher) and 1 % penicillin-streptomycin solution (Sigma-Aldrich). Cells were cultured in suspension for 12 days in a 37 °C and 5 % CO_2 atmosphere, performing sphere detachment and medium change every 3–4 days.

2.4. Cell viability assays

Panc02 and Panc02-L cell lines were seeded in 48-well plates (Thermo Fisher) at a density of 2.5×10^3 cells/well and incubated overnight. Then, they were exposed to different drugs (OLA (HY-10162, MedChemExpress, Princeton, New Jersey, USA), GMZ, Doxorubicin and Paclitaxel) at different concentrations during 72 h. Cells were fixed with cold trichloroacetic acid (TCA) (Sigma-Aldrich) for 20 min at 4°C and washed with distillated water (three times). After drying, cells were stained with Sulforhodamine B (SRB) (Sigma-Aldrich) diluted in 1 % acetic acid (20 min) at room temperature. After three washes with 1 % acetic acid, SRB was solubilized with Trizma® (10 mM, pH 10.5) (Sigma-Aldrich). Finally, the optical density (OD) of the dye was measured at 492 nm using Titertek Multiscan Colorimeter (Flow, Irvine, CA, USA). The percentage of proliferation was calculated as proliferation (%) = (sample OD/negative control OD) × 100. In addition, half-maximal inhibitory concentration (IC_{50}) was calculated using a non-linear regression analysis in GraphPad Prism 8 (GraphPad Software, CA, EEUU).

2.5. Quantitative Real-Time PCR

Mice tissues were preserved in RNAlater™ (Thermo Fisher) at − 80 °C. Subsequently, they were homogenized, and its RNA was extracted following the protocol described later. Cells were centrifugated and precipitate pellet was resuspended in TRI Reagent (Sigma-Aldrich) and mechanically homogenized for 15 s. Chloroform (0,2 volumes) (VWR international, Radnor, Pensilvania, EEUU) were added. After 15 min incubation at RT and 15 min centrifugation at 4 °C, the aqueous phase was obtained and mixed with 70 % ethanol (1:1 vol). RNA was extracted using RNeasy Mini Kit (Qiagen, Hilden, Germany) and quantified using Nanodrop 2000 (Thermo Fisher). Reverse transcription was performed using Reverse Transcription System kit (Promega, Madison, Wisconsin, EEUU) following the manufacturer's instructions. Finally, qPCR was performed using TB Green Premix Ex Taq II (Takara Bio, Kusatsu, Japan). The qPCR primers and annealing temperatures (Tm) used are listed in Table S1. Gene expression data were normalized using β2 microglobulin. All quantitative qPCR assays were performed in an ABI 7900 system (SeqGen, Torrance, CA, EEUU), and the 2−ΔΔCt method was applied to calculate relative expression levels.

2.6. Western blot assays

Cells were washed twice with PBS (phosphate-buffered saline) and lysed with RIPA lysis buffer (Sigma-Aldrich). Protein concentration was determined using Bradford Reagent (Bio-Rad, Hercules, California, EEUU). For electrophoresis, 40 μg of proteins from each sample were heated at 95 °C for 5 min and separated in 10 % SDS-PAGE gel. Fractions were transferred to nitrocellulose membranes (Bio-Rad), blocked for 1 h at room temperature in 5 % (w/v) milk powder in PBS containing 0.1 % Tween 20 (Bio-Rad) and co-incubated overnight at 4 °C with the primary antibodies: PARP1 1:2000 (Abcam, Cambridge, United Kingdom), γ-H2AX 1:1000 (Thermo Scientific) and β-actin-HRP 1:50,000 (Santa Cruz Biotechnology). Then, membranes were washed three times (0.1 % Tween 20 in PBS) and incubated (1 h) with the horseradish peroxidase conjugated (HRP) mouse anti-goat secondary antibody 1:5000 (Santa Cruz Biotechnology). Proteins were visualized using the ECL system (Little Chalfont, United Kingdom) in the LAS-4000 mini equipment (GE Healthcare, Chicago, Illinois, EEUU). Further analysis, as well as image processing and quantification of the bands, was performed using the program Quantity One analytical software (Bio-Rad, Hercules, CA). PARP1 and γ-H2AX expression were normalized relative to the β-actin level of the cell lines.

2.7. Radiosensitization assays

Cells were seeded in 6-well plate (Thermo Fisher) at a density of 5×10^4 cells/well. After 24 h, cells were treated with preOLA (Olaparib pretreatment, 5 μM) for 72 h. Then, cells were detached, seeded in 48-well plates $2{,}5 \times 10^3$ cells/well and incubated overnight. Cells were irradiated (8 Gy) and exposed to different GMZ concentrations for 72 h. Sulforhodamine B protocol was applied as previously described.

2.8. In vitro angiogenesis assay

Angiogenesis assays were carried out using human umbilical vein endothelial cells (HUVECs), which were purchased from the American Type Culture Collection (Rockville, MD, USA). HUVECs were cultured in 0.1 % gelatin-coated flasks in Endothelial Cell Growth Medium 2 (EGM-2) (Lonza Bioscence, Barcelona, Spain) supplemented with EGMTM-2 Endothelial SingleQuotes™ Kit (Lonza Bioscence) including FBS, human Fibroblast Growth Factor-Beta (hFGF-β), Vascular Endothelial Growth Factor (VEGF), R3-Insulin−like Growth Factor-1 (R3-IGF-1), human Epidermal Growth Factor (hEGF), ascorbic acid, hydrocortisone, heparin, and antibiotics (Sigma Aldrich, Madrid, Spain) at 37 °C in 5 % CO2 humidified atmosphere. To obtain the conditioned medium, Panc02 not treated or treated with OLA at 2 and 20 μM and Panc02-L cell line during 24 h was obtained. Subsequently, the culture medium is replaced by a fresh one, free of drugs, for 24 h. This medium was centrifuged at 12,000 rpm for 5 min, the supernatant being stored in an Eppendorf (conditioned medium) and stored at − 20 °C. Then, HUVECs were seeded in 96-well plates (5×10^4 cells/well) previously coated with Matrigel (50 μl) (Corning, New York, NY, USA) and were grown (12 h) in a medium without FBS. HUVECs were exposed to the conditioned medium. Calcein (Santa Cruz Biotechnology) was added to the cells, and the formation of tubes was visualized under optical and fluorescence microscopy at 3 h and 7 h. The images were analysed using ImageJ software with the Angiogenesis analyser plugin (NIH, USA), to evaluate the degree of microvascular network sprouting. Photos were taken using DM IL LED microscope (Leica, Wetzlar, Germany).

2.9. Cell migration assay

Before seeding, the Panc02 and Panc02-L cell lines were treated with 5 μM preOLA for 3 days. Cells were seeded in 12-well plate (Thermo Fisher) and grown to 95–100 % confluency in DMEM (Sigma-Aldrich) supplemented medium. The, a vertical gap was manually performed using a pipette tip [30]. Dead cells were remove using PBS and culture medium was substituted for DMEM without FBS to prevent cell proliferation. Then, OLA 2 μM was added to the wells and the cells were incubated for 72 h in which the migratory process was monitored using a DM IL LED microscope. The percentage of migration was calculated by measuring the area free of tumour cells at different times using the ImageJ software with the Chemotaxis and Migration Tool plugin (NIH, USA).

2.10. Colony formation assay

Both cell lines (Panc02 and Panc02-L) were treated with preOLA at a concentration of 5 μM for 3 days. After, the cells were detached and seeded in 12-well plate at 8×10^2 cells/well (Thermo Fisher) in DMEM supplemented medium and incubated overnight. In the following day, the cells were treated with OLA and GMZ for 72 h. The total growth time of the colonies from seeding was 7 days. After the colony formation period, the medium was removed, and wells were washed with PBS and fixed using 1 ml/well cold 70 % methanol (RT for 30 min) and subsequently washed again and dried. Colonies were stained using 0.5 % crystal violet (Sigma-Aldrich) diluted in 70 % methanol (1 ml/well) for 15 min. After three PBS washes, the plate was dried overnight, and the colonies were counted using ImageJ software.

2.11. ALDEFLUOR assay

Analysis of CSC-Ls was performed using ALDEFLUOR™ kit (StemCell Technologies, Vancouver, Canada). The test was carried out based on the information provided by the supplier. Briefly, cells lines were trypsinized, centrifuged (1800 rpm for 5 min) and resuspended in ALDEFLUOR assay buffer (8×10^5 cells/ml) and divided in two tubes (negative control and test). Aldehyde dehydrogenase inhibitor DEAB was added to the control tube (10 μl/ml) and then, both tubes were incubated with ALDEFLUOR reagent (5 μl/ml) at 37 °C for 40 min. Finally, cells were centrifuged (1800 rpm for 5 min) and resuspended in cold ALDEFLUOR buffer assay. Results were analysed using FACS Aria II (BD Biosciences, San Jose, USA) using FlowJo software. The gates were established using the DEAB-treated sample as a negative control.

2.12. DNA fragmentation assay (TUNEL)

TUNEL assay (Roche, Basel, Switzerland) was carried out on cells and sections of tumours from mice. Cells were seeded (5×10^4) in Culture Slides Chambers (Franklin Lakes, New Jersey, EEUU), incubated overnight, and treated with GMZ (1 μM), OLA (5 μM) and GMZ+OLA for

24 h. Cells treated with DMSO were used as control. Then, cells were fixed in paraformaldehyde (4 %) at RT for 1 h and washed with PBS. Tissue sections were deparaffinized with xylol and ethanol mixtures of decreasing concentrations (100, 95, 70 %) and rehydrated. Subsequently, both cells and tissues were permeabilized with Triton X100 (0.1 %) (Sigma-Aldrich) and sodium citrate solution diluted in PBS (0.1 %) for 2 and 8 min, respectively. After washing the samples with PBS, an experimental positive control was generated using 10 U/ml DNase I (Sigma-Aldrich) for 10 min at RT. Finally, TUNEL test was carried out following the manufacturer's instructions.

2.13. Cell cycle analysis

Cells were treated with preOLA (5 μM) for 72 h, trypsinized, centrifuged (1800 rpm for 5 min) and seeded in 6-well plate at a density of 2×10^5 cells/well (Thermo Fisher). After 24 h, the culture medium was removed, and a serum-free culture medium was added to arrest the cell cycle. Then, cells were treated with 5 μM OLA and 1 μM GMZ doses for 24 h. The protocol was carried out as in previous publications [31]. After incubation, cells were washed using PBS, detached, and centrifuged at 3500 rpm for 3 min. The supernatants were discarded, and the cellular pellets were resuspended (100 μl 4 °C PBS, 900 μl 70 % ethanol) and incubated 10 min at 4 °C. After that, cells were resuspended in PBS and the DNA was extracted using DNA extraction solution for 10 min (Na_2HPO_4 0.2 M diluted in 0.1 M acetic acid, pH 7.8). After removing DNA extraction solution by centrifugation (1500 rpm, 3 min), the pellets were processed using the PI/RNase Staining Buffer (BD BioSciences) at 37 °C for 15 min. Finally, pellets were washed and resuspended in 4 °C PBS, and the results were obtained in BD FACSCanto II flow cytometer (BD BioSciences) using FlowJo software.

2.14. Multicellular tumour spheroids formation and cytotoxicity assay

Cells were seeded in 6-well plate (Thermo Fisher) at a density of 5×10^4 cells/well. After 24 h, cells were treated with preOLA (5 μM) for 72 h. Therefore, control and presensitized with OLA cells were seeded in the 96-well plates (Thermo Fisher) (1×10^4 cells/well) previously coated with 50 μl of 1 % agarose to avoid the cell adhesion. Then, plates were centrifuged (10 min at 1800 rpm) to allow the aggregation of cells and formation of a single spheroid. After 24 h, the spheres were treated with GMZ in a range of concentrations and were incubating for 3 days. Photos of MTS were taken every day using DM IL LED microscope (Leica). Last day, cytotoxicity of MTS was measured using CCK-8 kit (Dojindo, Munich, Germany) following commercial instructions. Finally, the plates were read 450 nm using Titertek Multiscan Colorimeter (BertHold Technologies, Bad Wildbad, Germany) and the proliferation of treated wells was compared to the control. The percentage of proliferation was calculated as proliferation (%) = (sample OD/negative control OD) × 100. IC_{50} was calculated using a non-linear regression analysis in GraphPad Prism 8 (GraphPad Software, CA, EEUU).

2.15. In vivo assay

Female C57BL/6 mice (body weight: 20–25 g) (Charles River Laboratories Inc, Wilmington, MA, USA) were housed in colony cages with free access to water and food prior to the experiments and with controlled temperature, light and humidity (22 ± 2 ℃, 12 h light–dark cycle, 40–70 % relative humidity) and under specific pathogen-free conditions. Following our own experience, subcutaneous tumours were induced with the Panc02 and Panc02-L cell lines by injecting 5×10^5 cells in the right hind flank of mice in a total volume of 100 μl of saline. When the tumour was palpable, animals were randomly divided into six groups: Panc02 mice treated with OLA solvent (group I), GMZ (group II), OLA (group III), GMZ+OLA (group IV) and Panc02-L mice treated with OLA solvent (group V) and GMZ (group VI). GMZ was diluted in saline solution and OLA solvent was 5 % DMSO (D8418-1L, Sigma-Aldrich), 40 % PEG300 (HY-Y0873, MedChemExpress), 5 % Tween 80 (HY-Y189, MedChemExpress) and 50 % saline solution as indicated by the OLA's manufacturer. OLA and GMZ were administered in a dose of 50 mg/kg and 25 mg/kg respectively, both every three days up to a total of 10 cycles of treatment. The concentrations used were based on a previous *in vivo* study by our group using GMZ [29] and on other studies using OLA *in vivo* with a similar treatment regimen [32]. Weights and deaths were carefully recorded throughout the period. The following formula was used to calculate the tumour volume: V (mm^3) = ($a \times b^2 \times \pi$)/6, where "a" is the largest diameter of the tumour, and "b" is the largest diameter perpendicular to "a". Tumour growth values were measured in mm^3/day. In addition, mice survival was measured. After the experiments were completed, the mice were sacrificed with pentobarbital, and the tumours were excised. The *in vivo* study was approved by the Ethics Committee on Animal Experimentation of the University of Granada (Reference code: 16/01/2020/005) and in accordance with international standards (European Communities Council Directive 2010/63).

2.16. Histological analysis

Resected tumours were fixed in formaldehyde, included in paraffin, and cut with a rotation microtome (Leica, Wetzlar, Germany). After deparaffinization and hydration, the sections were stained with haematoxylin–eosin (Merck, Darmstadt, Germany).

2.17. Statistics

The statistical tests used were adapted to the data and were performed using SPSS v.15.0 software (SPSS, Chicago, IL, USA). Thus, for the general comparison between two samples, Student's t-tests were used. For the comparison between several samples, one-way (for univariate comparisons) and two-way ANOVA (for comparisons of two variables) were used, and Tukey's post-hoc test was performed. For the analysis of cytotoxicity assays, data were fitted following non-linear regression and logEC50 was calculated. Mice survival was evaluated with the Kaplan–Meier method. Finally, the log-rank test was used to compare the proportion of living mice between groups. Differences were considered statistically significant at a p-value < 0.05.

3. Results

3.1. PARP1 is overexpressed in Panc02 cells and its stable inhibition sensitizes tumour cell lines to drugs

As shown in Fig. 1A, *PARP1* mRNA was overexpressed in the Panc02 cell line 15-fold more than in mouse pancreatic tissue. Furthermore, a 6-fold inhibition of *PARP1* mRNA expression was demonstrated by qPCR in the Panc02-L cell line (Fig. 1B) which was generated using lentiviral PARP1 siRNA particles (see Methods). Inhibition of the expression of the PARP1 protein was demonstrated by Western Blot, confirming a 5-fold inhibition of PARP1 (Fig. 1C).

As shown in Fig. 1D, the Panc02-L line had a higher sensitivity to GMZ and OLA compared to the Panc02 line, in addition to other chemotherapeutic agents such as Paclitaxel and Doxorubicin. Specially, there was a 53.5 % decrease in the IC_{50} of GMZ (from 25.45 to 11.83 nM) and a 2.6-fold decrease in OLA (from 7.52 to 2.89 μM) (Fig. 1D). On the other hand, the combined treatment of GMZ and OLA in both lines induced a 35 % and 53 % decrease in the IC_{50} of GMZ in the Panc02 and Panc02-L lines, respectively (Fig. 1E and F). Furthermore, the combination of GMZ at concentrations of 10, 20 and 100 nM and OLA at 1 μM resulted in synergistic effects (IC<1) in all the conditions tested in both cell lines (Fig. 1G).

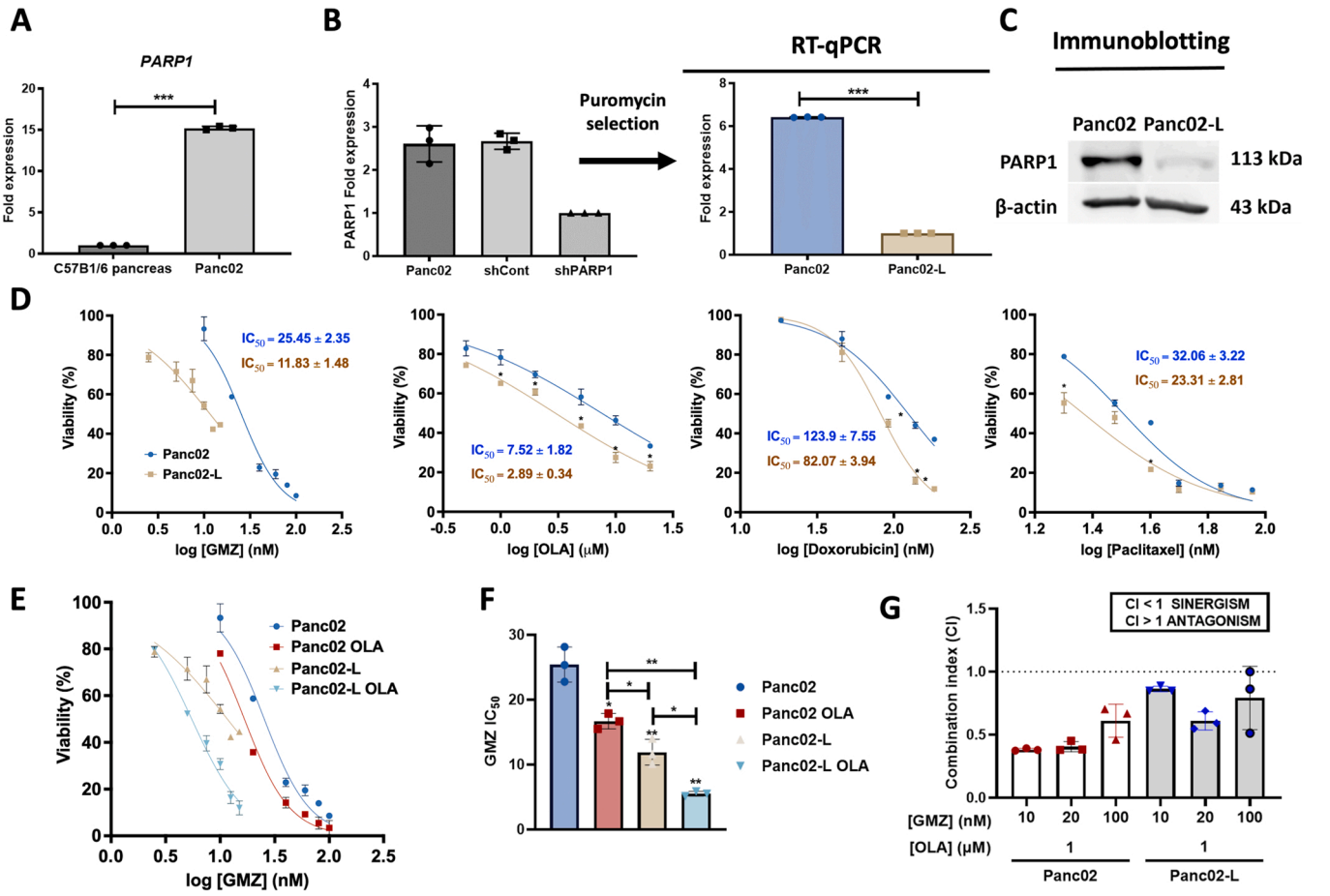

Fig. 1. PARP1 expression and drug cytotoxicity in Panc02 and Panc02-L tumour cell lines. (A) Quantification of *PARP1* mRNA expression in Panc02 cells compared to pancreatic tissue extracted from C57B1/6 mice. (B) Quantification of *PARP1* mRNA expression in Panc02, transfection control and Panc02-L cells after and before the cell selection with puromycin by qPCR (C) Quantitation of PARP1 protein expression by Western Blotting (β2-microglobulin and *β*-actin were used as control, respectively). (D) Cell sensitivity of Panc02 and Panc02-L cells to GMZ, OLA, Doxorubicin and Paclitaxel, and representation of their IC_{50} values. (E) Cell proliferation of Panc02 and Panc02-L cells exposed to OLA (1 *μM*+ GMZ simultaneously. (F) Graphical representation of the IC_{50} values obtained after treatments. (G) Graphical representation of the CI obtained after treating the Panc02 and Panc02-L lines with different concentrations of GMZ and OLA simultaneously. All data are presented as mean ± S.D of three independent experiments. *= $p \leq 0.05$, ** = $p \leq 0.01$, ***= $p \leq 0.001$.

3.2. Effects of Gemcitabine and Olaparib in PARP1 breakdown and apoptosis induction

To determine the possible correlation between GMZ and OLA treatments and PARP1 expression, an assay with PC cells exposed to both drugs was carried out. As shown in Fig. 2A, the exposure of Panc02 cells to a high GMZ dose (1 μM) for 24 h induced the PARP1 breakdown and degradation. However, pre-treatment with OLA (preOLA, 5 μM) prevented the typical degradation of PARP1 and its GMZ-related activation and degradation. In fact, densitometry analysis indicated a PARP1 accumulation after OLA and OLA-GMZ exposure. In addition, histone H2A.X (H2AX) phosphorylation is linked to the occurrence of DNA double-strand damage (genotoxicity) triggered by chemical agents or radiation [33]. The genotoxicity-inducing capacity of GMZ+OLA and GMZ associated to preOLA treatment (3 days), analysed through phosphorylated γ-H2AX, did not show significant differences in comparison to GMZ alone which induced 8- and 7-fold genotoxicity increase in Panc02 and Panc02-L cells, respectively, after 24 h of exposure (Fig. 2B and C). In addition, a TUNEL assay was carried out to determine the mechanism of action of GMZ and OLA against PC cells. Our results showed that GMZ at 24 h induced intense apoptosis in Panc02 cells. By contrast, OLA alone was unable to induce apoptosis. Finally, treatment with GMZ+OLA caused a high proportion of apoptotic nuclei. When Panc02-L cells (PARP1 inhibited) were analysed, it was found that GMZ treatment generated apoptotic nuclei in the cells in a similar way to the baseline cells (Fig. 2D and E). A cell cycle study demonstrated no significant cell cycle modification in Panc02 and Panc02-L cells after exposure to 1 μM GMZ, 5 μM OLA, or both simultaneously at 24 h. Only preOLA for 72 h induced a significant decrease in G0/G1, S and a slightly increase in G2/M phases in Panc02 cells. In contrast, Panc02-L cells showed an increase in the subG1 phase compared to baseline cells (from 2 % to 10 %) (Fig. 2F and G).

3.3. Pre-sensitization of pancreatic cancer cells by PARP1 inhibitors and radiotherapy increases antitumor drug effect

First, Panc02 and Panc02-L cell lines were treated using preOLA (IC_{50}). As previously described in Fig. 1, treatment with OLA was able to reduce the IC_{50} of GMZ by 35 % and 53 % in Panc02 and Panc02-L cells, respectively. A complementary study to increase pre-sensitization was performed in both Panc02 and Panc02-L cells using radiotherapy (IR) (8 Gy). After irradiating the cells, a significant 39 % reduction of IC_{50} GMZ was detected in Panc02 cells, while Panc02-L cells were resistant to this treatment (Fig. 3B and D). In addition, double pre-sensitization (preOLA+IR) induced a large reduction of the IC_{50} GMZ in Panc02 (46 %) and Panc02-L (40 %) cells (Fig. 3B and D). In fact, the greatest decrease in proliferation was detected in Panc02 cells after exposure to preOLA+IR (75 %). Panc02-L (*PARP1* inhibited) was comparatively less

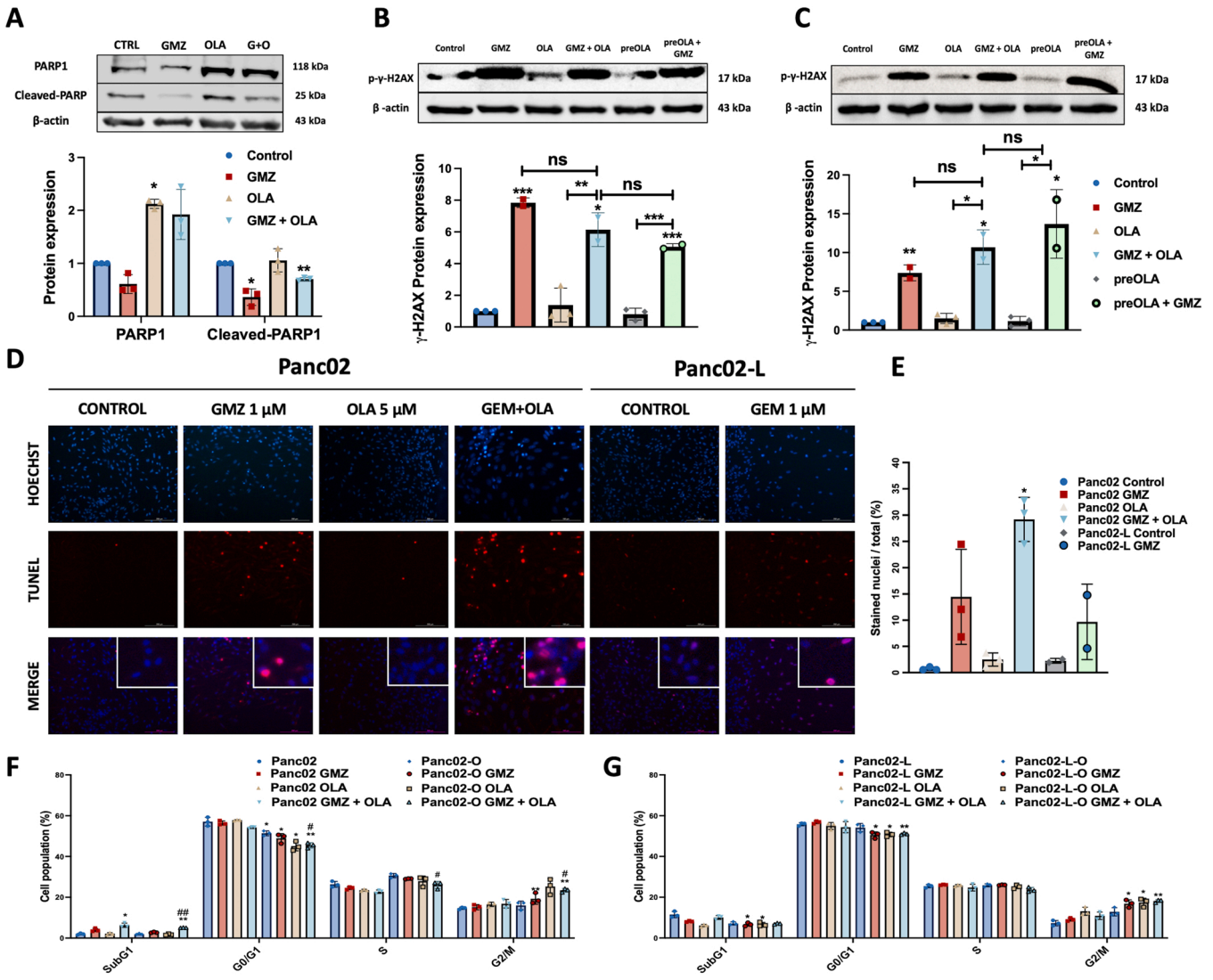

Fig. 2. PARP1 breakdown and apoptosis induction by GMZ and OLA. (A) Western Blot images and densitometry analysis of PARP1 and cleaved PARP expression in the Panc02 cells after exposure to OLA (5 μM; 72 h) and then GMZ (1 μM; 24 h). β-actin was used as control. (B) Western Blot images and densitometry of γ-H2AX protein expression and graphical representation of quantification in Panc02 and (C) Panc02-L tumour lines after treating cells with 1 μM GMZ and 5 μM OLA for 24 h. In addition, these lines were treated with preOLA for 72 h and subsequently treated with GMZ at the concentration described above. β-actin was used as loading control. (D) Representative fluorescence microscopy images of TUNEL assay. Nuclear marking was performed using the Hoechst stain. Photos were taken using 10X objective. (E) Graphical representation of the quantification of TUNEL-stained nuclei stained in comparation to the total nuclei. (F) and (G) Graphical representations of cell cycle analysis after carrying out a preOLA treatment for 72 h with 5 μM OLA in the cell lines Panc02 and Panc02L and subsequently treating with 1 μM GMZ, 5 μM OLA and both simultaneously for 24 h. (G) Data are presented as mean ± S.D. deviation of three independent experiments. ns = non-significant differences, *= $p \leq 0.05$, ** = $p \leq 0.01$, ***= $p \leq 0.001$ when the significant differences are compared to the experimental control. # = $p \leq 0.05$ when comparing the conditions with the basal cell line treated with preOLA.

affected by this preOLA treatment (50 % proliferation reduction) (Fig. S1).

Second, a clonogenicity assay corroborated a similar number of colonies of Panc02 cells sensitized with OLA (Panc02 OLA) and Panc02 without exposure to OLA (Fig. 2E). However, as shown in Fig. 2F, Panc02 cells treated with GMZ increased the number of colonies. This fact was not observed when Panc02 cells were pre-treated with OLA (Panc02 OLA). Furthermore, treatment with OLA and GMZ+OLA significantly reduced the number of colonies in Panc02 OLA cells.

Panc02-L cells significantly increased the number of colonies formed after treatment with GMZ, an effect that was not observed when pre-treated with OLA (Panc02-L OLA). However, a significant reduction in the number of colonies were observed in this line after treatment with OLA and GMZ + OLA (both in basal and pre-treated cells) during the clonogenic assay.

3.4. PARP1 inhibition reduces cell motility

A cell migration assay was performed to determine its modulation by PARP1 expression. As shown in Fig. 4A, migration of Panc02 cells was 48 % higher compared to Panc02-L cells. Furthermore, when Panc02 cells were exposed to OLA to inhibit PARP1 expression, a significant reduction (20 %) in migration was detected at 48 h. In contrast, Panc02-L cells exposed to the same OLA concentrations showed no variations in migration (Fig. 4A).

In addition, a migration test was carried out after pre-sensitization of both Panc02 and Panc02-L cells with OLA (5 μM). As shown in Fig. 4B and C, a significant modulation of the migration was observed in both cell lines. Furthermore, the use of GMZ IC_{25} (15 and 3.75 nM for Panc02 and Panc02-L cells respectively) promoted a significant decrease in migration of Panc02L cells at 48 h that was not observed in Panc02 cells.

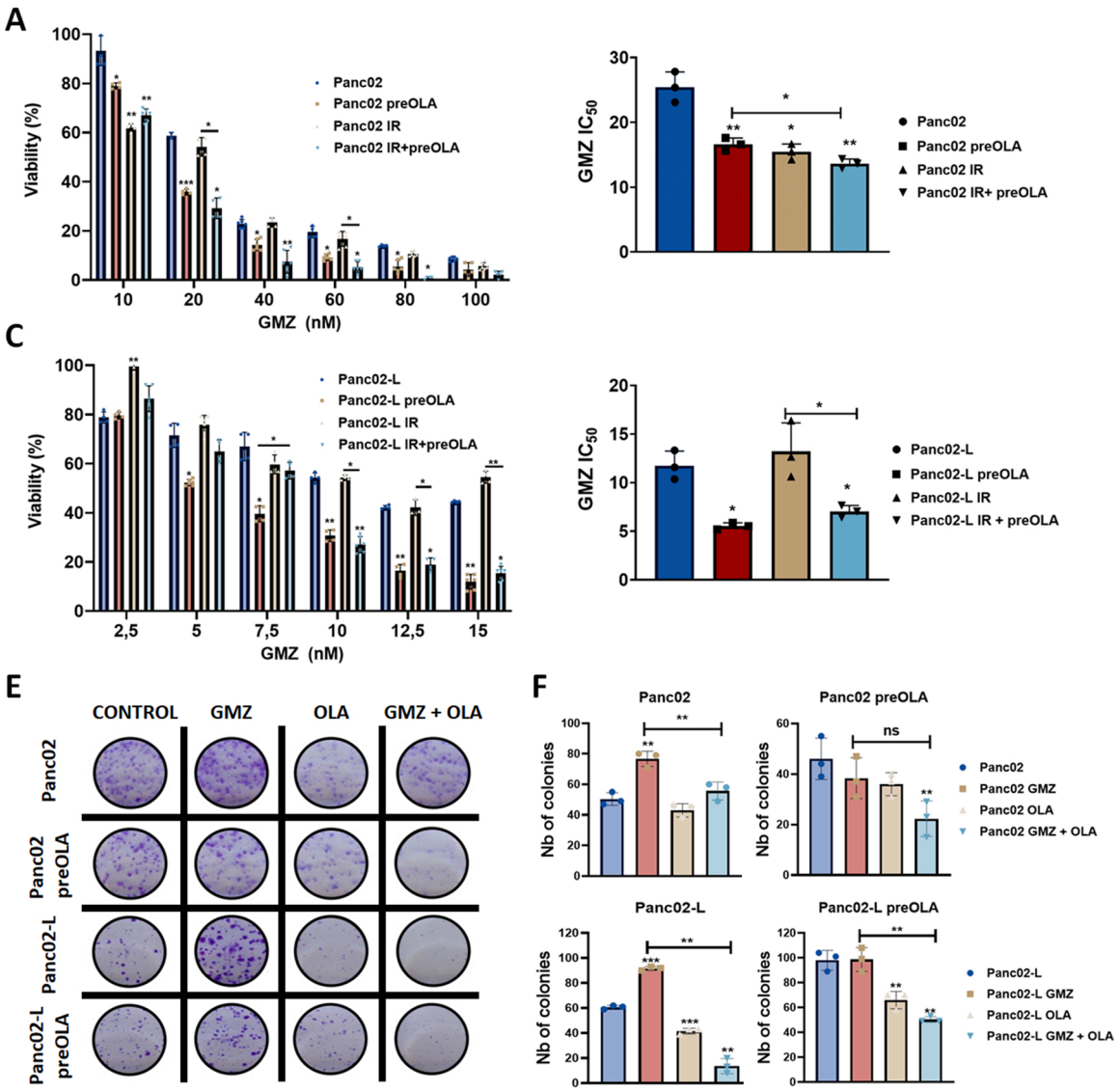

Fig. 3. Pre-sensitization of pancreatic cancer cells by radiotherapy and PARP1i. (A) Cell viability of Panc02 cells treated with preOLA (5 μM), IR (8 Gy) or pre-OLA+IR and treated with GMZ at different concentrations, and (B) graphical representation of the IC_{50} values obtained after the treatments. (C) Cell viability of Panc02-L cells treated with the same conditions previously described, and (D) graphical representation of the IC_{50} values obtained after treatments. (E) Representative images obtained from a clonogenic assay performed on Panc02 and Panc02-L cells after exposure to GMZ IC_{50} (25 and 12 nM respectively), OLA IC_{50} (7.5 and 3 μM respectively) or GMZ+OLA. (F) Graphical representation of the number of colonies formed in each of the conditions observed above. All data are presented as mean ± S.D of three independent experiments. ns = non-significant differences, *= $p \leq 0.05$, ** = $p \leq 0.01$, ***= $p \leq 0.001$.

Finally, OLA + GMZ treatment resulted in a significant decrease in migration at 48 h in both cell lines.

3.5. PARP1 inhibition modulates angiogenesis and sensitizes MTS to Gemcitabine

To determine the correlation between PARP1 expression in PC cells and the angiogenesis phenomenon, an assay using HUVEC cells was carried out. Fresh supernatants of Panc02, Panc02-L and Panc02 after treatment with OLA (0.2 and 20 μM) were obtained. HUVEC cells exposed to Panc02 cell line supernatant showed increased vessel formation compared to those exposed to supernatants from Panc02-L or Panc02 cells treated with OLA. All the variables studied in angiogenesis experiment, including number of junctions, length of the junction segments, and area of the mesh, among others, showed a significant reduction in the samples exposed to both Panc02-L and Panc02-OLA supernatants (Fig. 4D, E and S2). Moreover, MTS were generated from Panc02 and Panc02-L cells treated with preOLA before exposure to GMZ. As shown in Fig. 4D, pre-treatment with OLA increased the GMZ toxicity in both Panc02 and Panc02-L MTS. However, GMZ at all concentrations (1.5, 3, and 4.5 times the IC_{50} value, corresponding to 37.5, 75 and 112.5 nM in Panc02 and 18, 36 and 54 nM in Panc02-L) showed significantly higher toxicity in Panc02-L MTS compared to Panc02 (30 %, 46 % and 50 % respectively).

3.6. PARP1 inhibition decrease stem cell markers gene expression

On the other hand, a qPCR of CSC markers was performed to determine their modulation in relation to the expression of *PARP1*, and OLA and GMZ treatments. First, as shown in Fig. 5A, a greater decrease in the expression of *DNMT1* and *SOX2* was detected in Panc02-L relative to Panc02 cells. Second, both Panc02-L and Panc02 cells were treated with GMZ, OLA, and GMZ+OLA. As shown in Fig. 5B, the expression of *DNMT1* and *SOX2* increased when cells were treated with both drugs. In addition, a significant increase in *PARP1* expression was observed. Furthermore, simultaneous exposure to GMZ+OLA further decreased

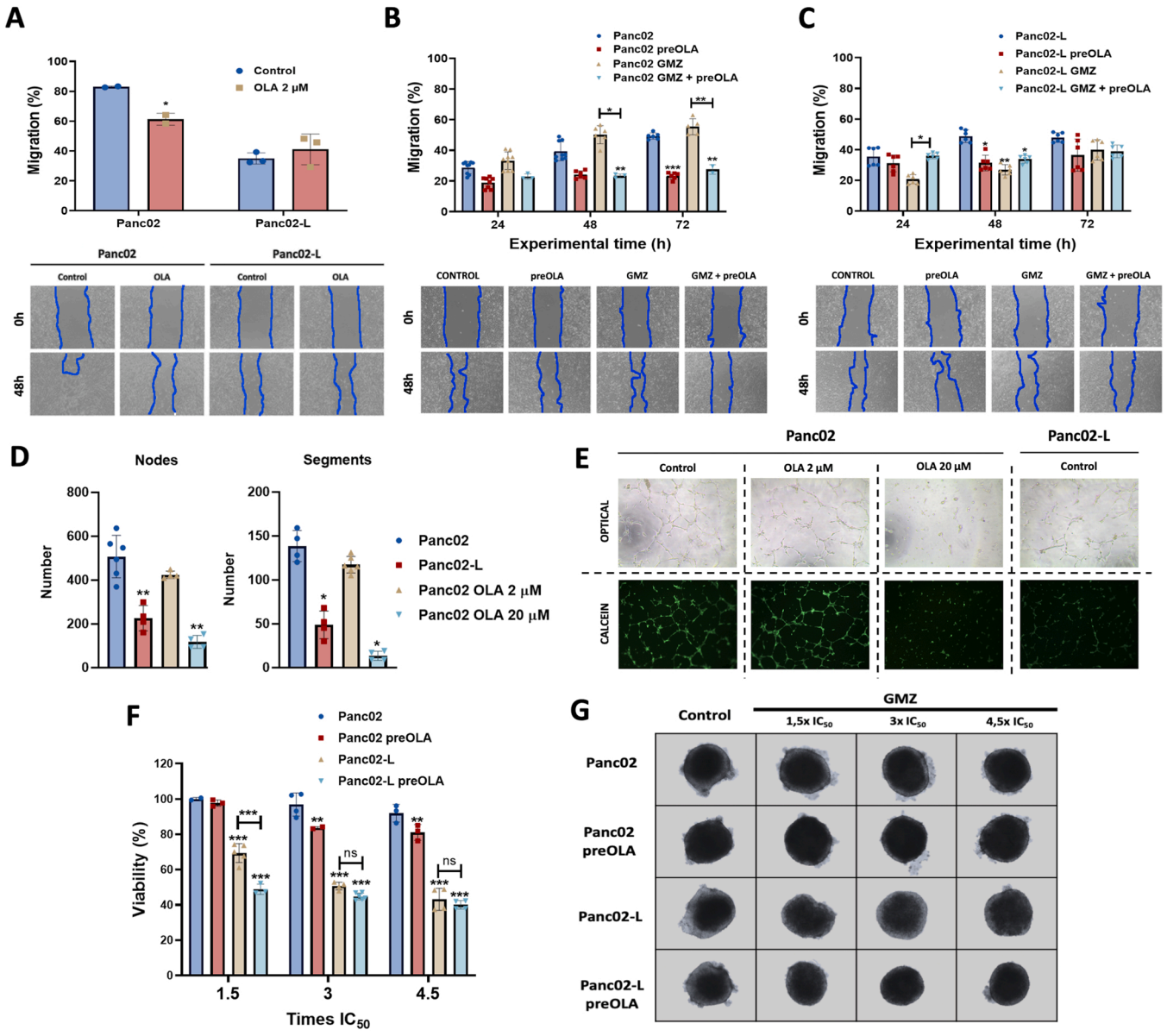

Fig. 4. Influence of PARP1 inhibition on tumour aggressivity. (A) Graphical representation and representative images of the relative (%) Panc02 and Panc02-L cell migration after 48 h of exposure to OLA (2 μM). Images were taken 0 and 48 h after exposure to drugs (B) Graphical representation and representative images of the relative (%) Panc02 and (C) Panc02-L cell migration after pre-treatment with OLA (5 μM, preOLA) and treatment with GMZ IC_{25} (15 and 3.75 nM respectively) for 3 days. Images were taken 0 and 48 h after exposure to drugs. (D) Graphical representation of two angiogenic parameters (nodes and segments) analysed from the images obtained using light microscopy. Random visual field photos were obtained from the replicates and analysed using ImageJ. (E) Representative optical and fluorescence microscopy images of blood vessel formation by HUVECs cells after exposure to conditioned media obtained from Panc02, Panc02-L and Panc02 cells exposed to OLA (2 and 20 μM) and incubation with calcein. Photos were taken using 4X objective. (F) Graphical representation of the viability of MTS from Panc02 and Panc02-L cells after preOLA and GMZ treatments. (G) Representative light microscope images of MTS after treatment using 4X magnification (3 days after treatment). Data are presented as mean ± S.D. of three independent experiments. *= $p \leq 0.05$, ** = $p \leq 0.01$, ***= $p \leq 0.001$.

DNMT1 and *PARP1* compared to the drugs alone in Panc02, while in Panc02-L a similar behaviour was observed but increasing the expression of *SOX2* compared to individual treatments.

3.7. Cancer stem-like cells from pancreatic cancer show a different sensitivity to GMZ

After observing modulation in the expression of two CSC markers by stable inhibition of PARP1, CSC-Ls from Panc02 and Panc02L cells were induced and characterized using the ALDEFLUOR protocol (see methods). As shown in Fig. 5C, a 10 % and 23 % increase was observed in Panc02 and Panc02L cells, respectively, with expression of high levels of this enzyme. To determine the sensitivity of CSC-Ls to GMZ, these cells were exposed to different concentrations of the drug. Interestingly, as shown in Fig. 5D, a significant reduction in the IC_{50} of GMZ was detected in both CSC-Ls derived from Panc02 and Panc02-L cells (0.4 and 2 μM, respectively) relative to baseline cells (25 and 12 nM respectively). Determination of *PARP1* by qPCR showed similar expression levels in both CSC-L and Panc02 basal cells. Surprisingly, Panc02-L CSC-Ls showed 45-fold higher *PARP1* expression than Panc02-L basal cells. In addition, GMZ at high concentration (1 μM), induced a significant increase in the expression of *PARP1* in both Panc02 and Panc02-L basal cells (12.5- and 26-fold, respectively) but not in CSC-Ls from Panc02 and Panc02-L cells where the drug only induced a slight increase (3.3-fold) or even decrease in *PARP1* expression, respectively (Fig. 5E). Furthermore, CSC-L spheres derived from Panc02 were

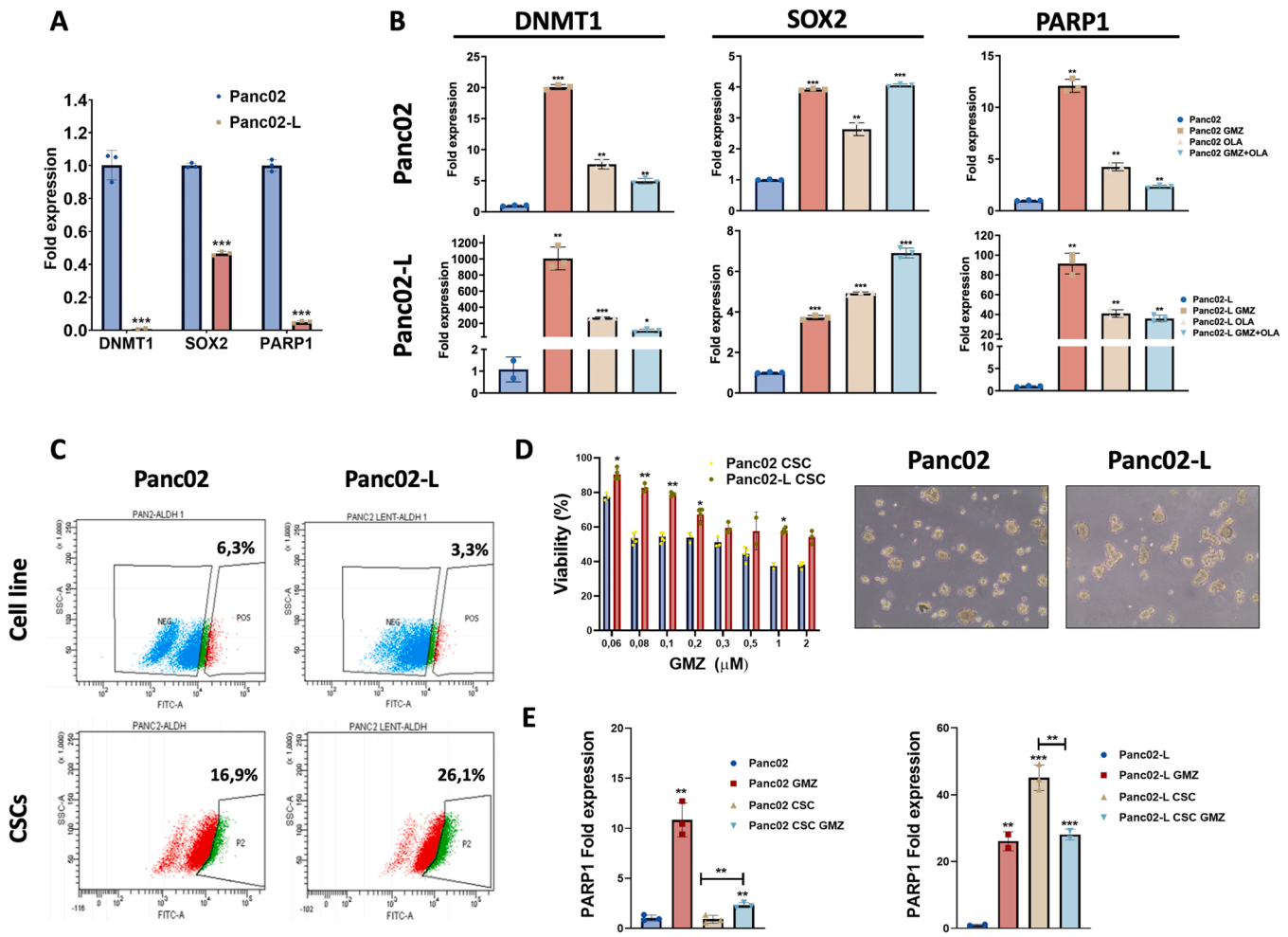

Fig. 5. CSC-L characterization. (A) Comparative RT-qPCR analysis of CSC markers (*DNMT1 and SOX2*) and of *PARP1* expression between Panc02 and Panc02-L cell lines and (B) analysis of the same markers in both cell lines after GMZ IC_{50} (25 and 12 nM respectively), OLA IC_{50} (7.5 and 3 μM respectively) or GMZ+OLA treatments for 3 days. (C) Panc02 and Panc02-L CSC-Ls were isolated and analyzed using the ALDEFLUOR protocol to ensure its enrichment in stem cells. The aldehyde dehydrogenase inhibitor DEAB was used to establish base fluorescence which is interpreted as dim cells for ALDEFLUOR. (D) Verification of the cytotoxicity of the CSC-L cells isolated from both cell lines against the drug GMZ. Representative images at light microscope of the CSC-Ls obtained from the lines Panc02 and Panc02-L. (E) Quantification of *PARP1* gene expression by RT-qPCR of basal cells and CSC-Ls derived from untreated Panc02 and Panc02-L lines or being treated with GMZ 1 μM for 24 h. Data are presented as mean ± S.D. of three independent experiments. *= $p \leq 0.05$, ** = $p \leq 0.01$, ***= $p \leq 0.001$.

characterized by qPCR analysing the *MRD1* (p-glycoprotein) marker, involved in DNA damage resistance, which was found to be 2-fold higher in these cells. However, when they were cultured again in DMEM medium, the expression of this marker returned to its basal levels (Fig. S3A).

3.8. GMZ-induced pancreatic cancer cells selection

We wanted to analyse the ability of GMZ and OLA to select populations with different expression of PARP1. The results obtained (Fig. S3B) indicated that the Panc02-L line was correctly silenced. Furthermore, the use of OLA at slightly cytotoxic (IC_{25}, 2μM) and highly cytotoxic (IC_{50}, 7.5 μM) doses selected populations with lower expression of PARP1. The use of GMZ IC_{25} (15 nM) dose selected populations with higher (2-fold) expression at the mRNA level, although the IC_{50} dose decreased its expression in the cells. Finally, we observed that the combined treatment with GMZ and OLA at IC_{25} concentrations allowed obtaining populations that expressed 40 % less PARP1 with respect to the Panc02 line.

To demonstrate that GMZ was capable of selecting cells with CSC characteristics, a high dose of GMZ (1 μM) was used. As shown in Fig. S3C, after treatment with GMZ, a population with high expression of markers of CSC phenotype (*CD24*, *CD44*, *CD133*, *SOX2*, *DNMT1*) was detected. Furthermore, these cells showed higher expression of *PARP1* and *BRCA1* (9- and 4-fold respectively).

3.9. Pharmacological and stable inhibition of PARP1 decreases the proliferation of tumours derived from pancreatic adenocarcinoma cell lines in vivo

Tumours from Panc02 and Panc02-L cells were generated to verify the antitumor effect of the treatments tested *in vitro*. First, as shown in Fig. 6A, the tumours generated from the Panc02-L line showed a significant 62 % growth reduction compared to those generated from Panc02. In addition, as illustrated in Fig. 6B, both GMZ and OLA treatments significantly decreased the volume of the tumour induced with Panc02 cells from the eighth treatment cycle (day 24), reaching a significant reduction of 70 % and 64 %, respectively. Furthermore, treatment with GMZ+OLA was effective one cycle earlier (day 21) and achieved a higher decrease in tumour volume (86 % *versus* control) compared to GMZ or OLA alone (Fig. S4A). In addition, treatment of Panc02-L tumours with GMZ significantly inhibited their growth by 63 % (Fig. 6D). This behaviour was like that observed with GMZ+OLA in Panc02 cells (Fig. S4B). On the other hand, as shown in Fig. 6E, the

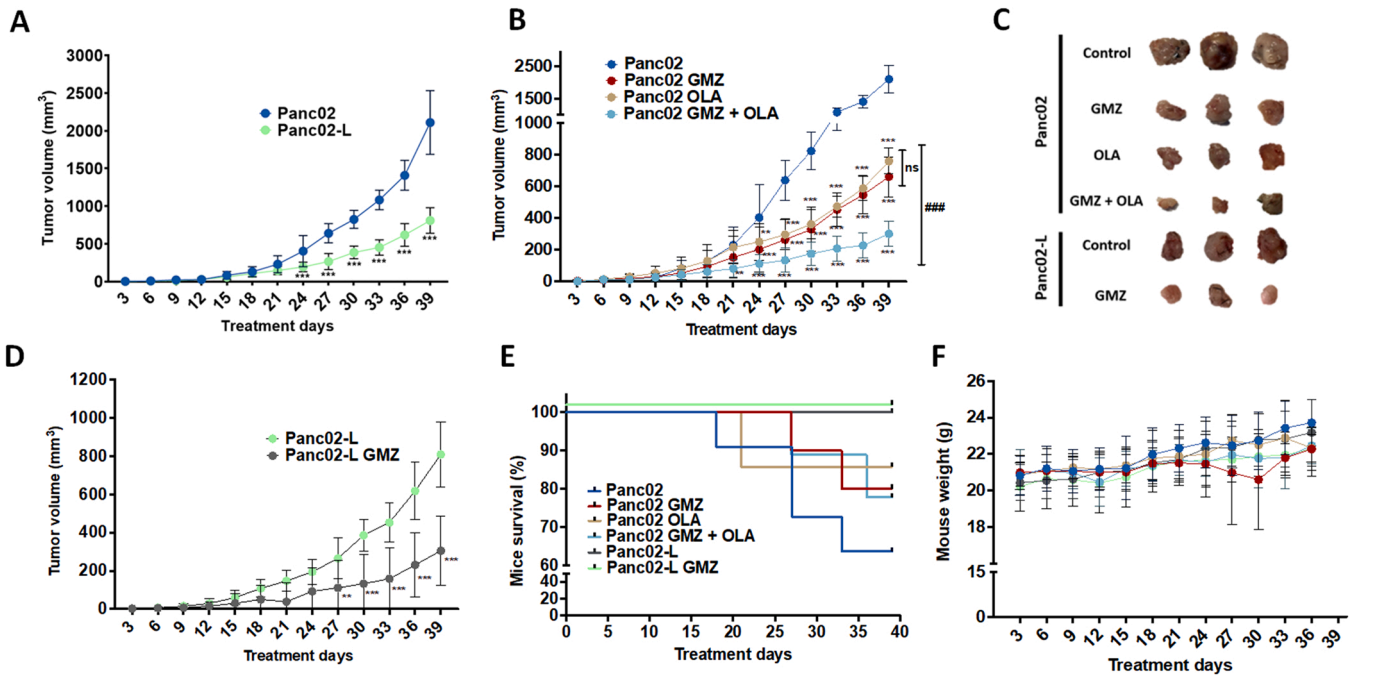

Fig. 6. Panc02 and Panc02-L *in vivo* assays. (A) Graphical representation of tumor volume growth induced from the Panc02 and Panc02-L cell lines. (B) Graphical representation of pancreatic tumor volume growth in C57BL/6 mice generated from the Panc02 and (D) Panc02-L cell lines. Mice were treated with GMZ, OLA and GMZ+OLA. Untreated mice were used as controls. (C) Illustrative images of tumors obtained in all experimental groups after the end of the experiment. (E) Graphical representation (Kaplan-Meier test) of mice survival after 39 days of experiment. (F) Graphical representation of the weights of the mice measured in each of the treatment cycles. Measurements were taken every 3 days and monitored for 39 days. Data are presented as mean ± SD (n = 10). Significant inhibition of tumor growth comparing treatments (# = $p \leq 0.05$, ## = $p \leq 0.01$, ### = $p \leq 0.001$), and comparing treatments with control (* = $p \leq 0.05$, ** = $p \leq 0.01$, *** = $p \leq 0.001$).

survival of control Panc02 mice was the lowest, followed by the different treatment groups (GMZ, OLA and GMZ+OLA). Furthermore, all mice bearing tumours induced from Panc02-L survived although the analysis using Kaplan-Meier did not show significant differences. Finally, no significant differences were observed in mice weights between experimental groups (Fig. 6F).

3.10. Histological and gene analysis of excised tumours

After the end of the experiment, mice were dissected, and tumours were removed and processed. A TUNEL test was carried out to detect death by apoptosis in the tumor sections obtained. As shown in Fig. 7A, early apoptotic zones were observed in control Panc02 tumors, while apoptosis was lower in tumors treated with GMZ and GMZ+OLA. In addition, large induced apoptosis was observed in control Panc02-L tumors, while it was significantly lower in those treated with GMZ.

The analysis of tumour RNA by RT-qPCR (Fig. 7B) showed that all applied treatments significantly decreased *STAT3* expression, which was higher with the use of GMZ+OLA (80 %) than in treatments alone (30 % and 40 % with GMZ and OLA, respectively). The Panc02-L line underwent an 80 % inhibition compared to the Panc02 line, while its expression in GMZ-treated tumours was similar. In contrast, *EPCAM* expression was significantly increased after all treatments in both Panc02 and Panc02-L tumours. Only in Panc02 tumours treated with GMZ+OLA was a significant reduction (70 %) of *EPCAM* detected. In addition, *MDR1* expression was significantly decreased after all treatments compared to untreated tumours. Only Panc02-L tumours treated with GMZ showed no significant differences compared to the control group.

For the rest of the genes analysed (*KI67*, *PARP1* and *EGFR*), a significant decrease in expression was detected in all treated tumours compared to untreated tumours. Interestingly, the expression of *KI67* and *PARP1* in Panc02 tumours was significantly lower after treatment with GMZ+OLA compared to individual treatments (GMZ or OLA). In the case of Panc02-L tumours, a decrease in the expression of *KI67*, *PARP1* and *EGFR* was observed (70 %, 65 % and 80 %, respectively) after all treatments.

4. Discussion

The aggressiveness and lethality of PC, the fourth leading cause of cancer death in both men and women [34], requires the development of new therapeutic strategies [35]. Despite the relevance of PARP inhibitors in the treatment of this cancer, most patients still do not benefit from these drugs [9,36]. In fact, the resistance of cancer cells to PARP inhibitors is one of their main limitations [37]. In this context, it is necessary to increase knowledge about the role of PARP1 in PC, the effect of PARP1 inhibition on the development of this tumour, and the *in vivo* effect of PARP1 inhibition, both alone and in combination with GMZ, the drug of choice in this type of cancer.

Our results showed that, unlike healthy pancreatic tissue from C57BL/6 mice, the Panc02 PC cell line, derived from the same murine strain, expressed very high levels of *PARP1*, making it an ideal candidate for our experiments. Furthermore, stable inhibition of *PARP1* in these cells was successful, developing a new modified cell line (Panc02-L) with virtually no expression of PARP1 which was sensitized against several drugs (Gemcitabine, Doxorubicin and Paclitaxel). Our results supported previous studies showing a significantly higher sensitivity of PARP-inhibited cell line to cytotoxic drugs (GMZ, Paclitaxel and Cisplatin) compared to the wild-type cell line. This suggested that PARP1 expression is relevant to the efficacy of these antitumor drugs in PC cells. Although PARP1 inhibition had not been previously linked to drug sensitization in PC, Mintz et al. [38] recently demonstrated that stable inhibition of *PARP1* by CRISPR/Cas9-sensitized breast cancer cells to GMZ, Doxorubicin, and Docetaxel. Moreover, the use of PARP1i was able to sensitize drug-resistant gastric cancer cells to Cisplatin,

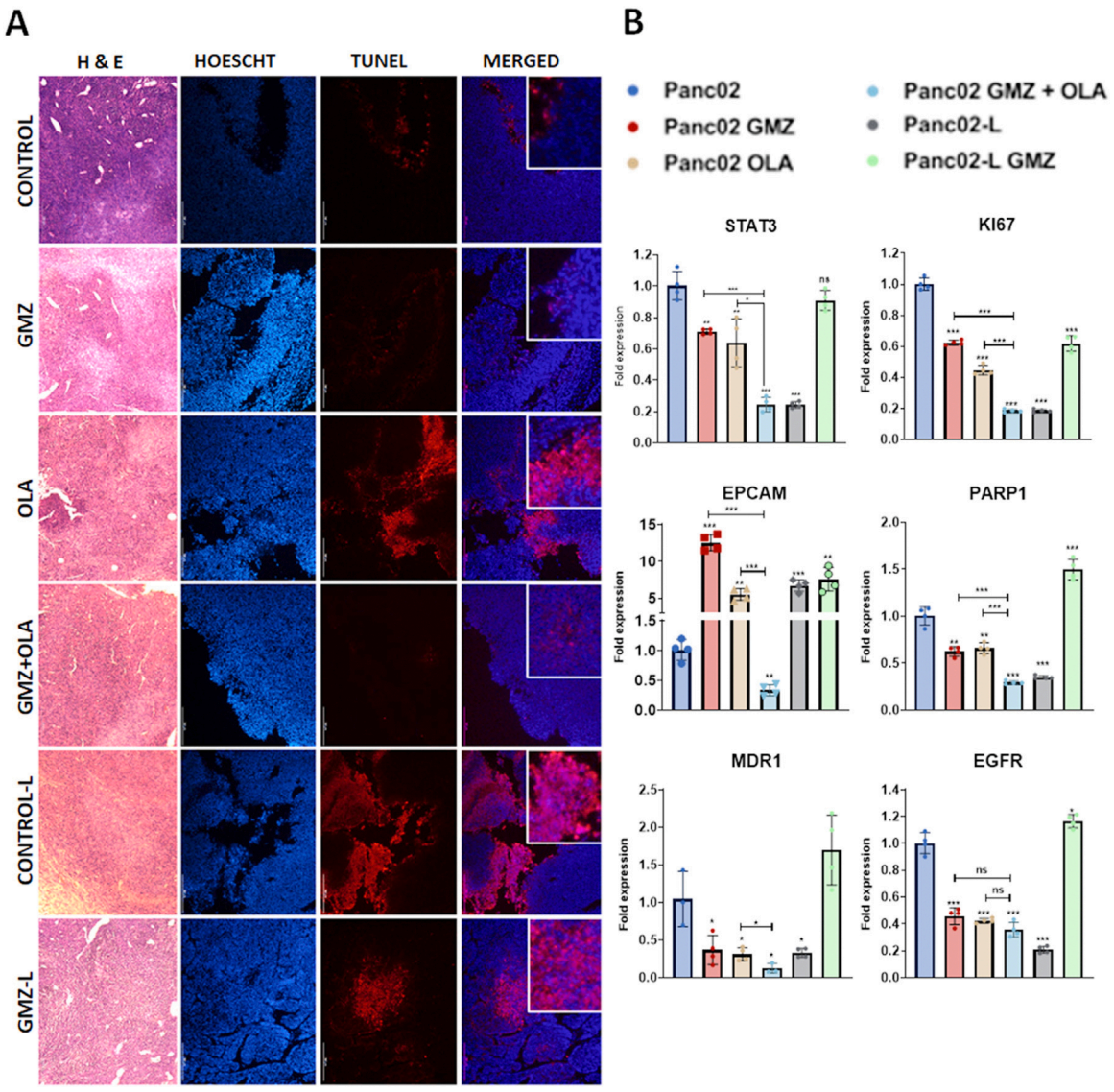

Fig. 7. Histological and gene expression analysis of tumours. (A) Histological evaluation of haematoxylin-eosin staining and apoptosis in resected tumours by TUNEL assay. Representative photographs of tumour sections derived from Panc02 and Panc02-L cells before (control) and after GMZ, OLA and GMZ+OLA treatments, showing TUNEL-positive cells (red). Sections were counterstained with Hoechst (blue). Photographs were taken at 10X magnification; (B) RT-qPCR analysis of *STAT3, EPCAM, MDR1, KI67, PARP1* and *EGFR* gene expression. Data are presented as mean ± SD of three independent experiments. Statistical differences are represented as *= $p \leq 0.05$, ** = $p \leq 0.01$, ***= $p \leq 0.001$.

non-small cell lung cancer cells to GMZ, and uterine and ovarian cancer cells to Carboplatin and Cisplatin [39–41]. Our results clearly indicate that the exposure of PC cells to OLA, including in Panc02-L cell line, increased their sensitivity against antitumor drugs. In this cell line, the extra sensitization effect exerted by OLA may be due to the inhibition exerted on PARP1 that remains expressed, in addition to the effect that OLA has against two other PARP enzymes such as PARP2 and tankyrase-1. Accordingly, this PARP1i decreased the IC_{50} of GMZ by 35 % in Panc02 cells and by 53 % in the modified Panc02-L line. In the latter cell line, OLA induced a synergistic effect, resulting in an 80 % decrease in the IC_{50} of GMZ compared to the Panc02 basal cell line. This synergistic effect may be due to the effect of both drugs on PARP1: Olaparib inhibits PARP1 activation by preventing the PARylation and its ability to repair damage while GMZ would degrade PARP1 through its cleavage (by activation) and autophagy, as previously described by Wang et al. [42]. Although most of the of studies focusing on PARP inhibitors are performed with BRCA-deficient cell lines, it is known that the effect of PARP1 inhibitors such as Olaparib can exert their effect through other alternative routes to the deficiency in homologous recombination, such as the inhibition of single-stranded damage repair (inhibiting SSBR), inhibiting the formation of fork stalling in the DNA repair process, causing PARP trapping or also preventing the transcription of important oncogenes such as p53 or NF-kB [14]. Furthermore, the *in vitro* combination of irradiation (8 Gy) and OLA (*i.e.*, inhibition of PARP1) further increased the sensitivity to GMZ in the Panc02 and Panc02-L cell lines, decreasing their proliferation capacity. These results were supported by a colony formation assay in which both Panc02 and Panc02-L cells exhibited decreased proliferation and colony formation capacity with respect to a basal sample after sensitization with OLA, also preventing the selection of more resistant and aggressive cells by GMZ.

On the other hand, the study of vessel formation in the HUVEC cell line using conditioned media obtained in Panc02 cells treated with OLA and in Panc02-L indicated that the inhibition of PARP1 in these tumour lines prevented the induction of angiogenesis *in vitro* in a dose-dependent manner. Accordingly, one of the factors that could explain

the relevance of PARP1 in tumour progression should be related to an increase in the angiogenic capacity of tumour cells, with the subsequent ability to form a greater number of blood vessels nearby that rapidly increased its irrigation and proliferation. Of note, the capacity of tumour cells to release angiogenic factors that induce tumour progression and its negative relationship with PARP1 inhibition have been demonstrated in previous studies [43]. It was surprising to find that the modified Panc02-L line had a lower expression of two CSC markers (*DNMT1* and *SOX2*), which would indicate that inhibition of PARP1 decreased the aggressiveness of this pancreatic tumour line. Analysis of these markers in the cell populations treated with GMZ and OLA showed that treatment with high doses of both drugs can select more aggressive populations because these cells can survive them. Such selection of cell populations by GMZ has been described in previous works which indicated that the drug selects more invasive populations and, in addition, generates a pro-survival response [44,45].

Cell motility is an important process for a tumour cell to move through its environment and may be involved in the initiation of a metastatic process because it is a necessary condition for the cell to reach a blood vessel and spread throughout the body. In PC, no relationship between cell motility and PARP1 has been described. Our results showed that the stable inhibition of PARP1 and by OLA induced a significant decrease in the migratory capacity of Panc02 cells. In fact, pre-treatment with OLA decreased the migratory capacity in both cell lines, while the administration of GMZ IC_{25} (15 nM) induced a slight boosting effect of the migration process in the Panc02 line. Conversely, the administration of GMZ IC_{25} (3.75 nM) in the Panc02-L line was cytotoxic, significantly decreasing migration. Similar results were previously described in ovarian cancer, cervical cancer and hepatocellular carcinoma [46–48]. This decrease in the migratory ability of tumour cells due to the inhibition of PARP1 could be exploited to prevent the formation of possible metastases by administering PARP1 inhibitors in early-stage tumours.

Regarding the mechanism of action of GMZ and OLA in PC, our results indicate that GMZ causes a depletion of the PARP1 available in the cell to repair DNA damage, while OLA prevented the effective processing of PARP1 and its activation. These results were supported by treatment with high doses of GMZ in conjunction with OLA, capable of inducing extensive DNA fragmentation during the apoptotic process. In addition, pre-treatment with OLA for 72 h induced cell cycle arrest in S and G2/M phases in the Panc02 line, which was less conspicuous in the Panc02-L cell line. Both pre-treatment with OLA and stable inhibition in this line induced a greater sensitivity to GMZ in three-dimensional MTS, which supports the previously described results. This OLA-induced cell cycle arrest has been previously described in pancreatic and gastric cancer [49,50].

Previous *in vivo* studies demonstrated that stable PARP1 inhibition in PC3 (prostate cancer) tumour cells produced decrease in the tumour progression and volume (a 70 %) [51]. In addition, the administration of nanoparticles containing siRNAs against PARP1 resulted in an increase in the survival of murine Brca1-deficient ovarian cancer cells [52]. On the other hand, treatment with Olaparib (50 mg/kg) and Gemcitabine (40 mg/kg) (two days) followed by exposure to 10 Gy of photons or protons significantly inhibited the growth of tumours generated in immunosuppressed mice using the MIA cells PaCa2 pancreatic cancer cell line [53]. Our *in vitro* results were supported by *in vivo* tests performed in C57BL/6 mice, where combined treatment with GMZ+OLA reduced tumour growth. Moreover, tumours derived from the modified Panc02-L line showed significantly lower growth than those from the basal cell line, supporting the influence of PARP1 in the progression of PC. Notably, none of the Panc02-L cell-derived tumour mice died over the 39 days of treatment, while deaths occurred spontaneously in all Panc02 groups. Results of Kaplan-Meier analysis did not change despite *in vivo* experience stop by the high tumour size increase in control mice. This suggests that Panc02-L cells show lower aggressiveness, which was supported by *in vitro* assays in which we detected a lower capacity for migration, angiogenesis, and proliferation (MTS experiments). These effects were also reflected in tumour tissue where treatments and stable inhibition of PARP1 (Panc02-L) reduced the expression of genes involved in cell proliferation (*KI67*), angiogenesis and metastasis (*STAT3* and *EGFR*), cell detoxification (*MDR1*) and DNA damage repair (*PARP1*). Finally, treatment with GMZ induced small apoptotic areas in tumour tissue, while treatment with OLA and stable PARP1 inhibition resulted in large apoptotic areas, suggesting that the latter altered the DNA damage repair process, leading to DNA fragmentation.

5. Conclusions

Our study demonstrated that the expression of PARP1 plays a relevant role in the tumour progression of PC since its stable inhibition (Panc02-L) as well as the use of a PARP inhibitor (OLA) were able to increase the sensitivity of PC cells to GMZ in both two- and in three-dimensional models (MTS), significantly reducing colony formation, cell migration, and angiogenesis. Furthermore, stable inhibition of PARP1 decreased the expression of CSC markers, which may be related to lower aggressiveness. These results were corroborated *in vivo*, where the combined treatment of GMZ+OLA significantly inhibited and reduced tumour growth and 100 % survival was observed in Panc02-L cell-derived tumours compared to tumours derived from the baseline cell line.

CRediT authorship contribution statement

Francisco Quiñonero: Investigation, Formal analysis, Writing – original draft. **Cristina Mesas:** Investigation, Formal analysis. **Jose A. Muñoz-Gámeza:** Investigation, Formal analysis. **Cristina Jiménez-Luna:** Formal analysis. **Gloria Perazzoli:** Investigation, Software. **Jose Prados:** Conceptualization, Writing – original draft. **Consolación Melguizo:** Conceptualization, Writing – original draft. **Raul Ortiz:** Conceptualization, Writing – original draft.. All authors reviewed the manuscript and provided comments or suggestions. All authors read and approved the final manuscript.

Acknowledgements

This work was supported by the Project Innbio INB-009 (Granada University and ibs. GRANADA), Project DTS17/00081 (Instituto de Salud Carlos III) and by the CTS-107 Group and Projects A-CTS-666-UGR20 and B-CTS-122-UGR20 of the Junta de Andalucía (FEDER) (Spain). FQ acknowledges the FPU2018 grant from the Ministerio de Educación, Ciencia y Deporte y Competitividad (Spain). We thank Instrumentation Scientific Center (CIC) from University of Granada for technical assistance.

Conflict of interest statement

The authors declare no conflict of interest.

Appendix A. Supporting information

Supplementary data associated with this article can be found in the online version at doi:10.1016/j.biopha.2022.113669.

References

[1] H. Sung, J. Ferlay, R.L. Siegel, M. Laversanne, I. Soerjomataram, A. Jemal, F. Bray, Global cancer statistics 2020: GLOBOCAN estimates of incidence and mortality worldwide for 36 cancers in 185 countries, CA Cancer J. Clin. 71 (2021) 209–249, https://doi.org/10.3322/caac.21660.

[2] J. Huang, V. Lok, C.H. Ngai, L. Zhang, J. Yuan, X.Q. Lao, K. Ng, C. Chong, Z. J. Zheng, M.C.S. Wong, Worldwide burden of, risk factors for, and trends in pancreatic cancer, Gastroenterology 160 (2021) 744–754, https://doi.org/10.1053/J.GASTRO.2020.10.007.

[3] A. McGuigan, P. Kelly, R.C. Turkington, C. Jones, H.G. Coleman, R.S. McCain, Pancreatic cancer: a review of clinical diagnosis, epidemiology, treatment and

outcomes, World J. Gastroenterol. 24 (2018) 4846–4861, https://doi.org/10.3748/wjg.v24.i43.4846.
[4] L.A. Daamen, V.P. Groot, M.P.W. Intven, M.G. Besselink, O.R. Busch, B. G. Koerkamp, N.H. Mohammad, J.J. Hermans, H.W.M. van Laarhoven, J. J. Nuyttens, J.W. Wilmink, H.C. van Santvoort, I.Q. Molenaar, M.W.J. Stommel, Postoperative surveillance of pancreatic cancer patients, Eur. J. Surg. Oncol. 45 (2019) 1770–1777, https://doi.org/10.1016/J.EJSO.2019.05.031.
[5] M.N. Rosen, R.A. Goodwin, M.M. Vickers, BRCA mutated pancreatic cancer: a change is coming, World J. Gastroenterol. 27 (2021) 1943–1958, https://doi.org/10.3748/wjg.v27.i17.1943.
[6] T. Conroy, P. Hammel, M. Hebbar, M. Ben Abdelghani, A.C. Wei, J.-L. Raoul, L. Choné, E. Francois, P. Artru, J.J. Biagi, T. Lecomte, E. Assenat, R. Faroux, M. Ychou, J. Volet, A. Sauvanet, G. Breysacher, F. Di Fiore, C. Cripps, P. Kavan, P. Texereau, K. Bouhier-Leporrier, F. Khemissa-Akouz, J.-L. Legoux, B. Juzyna, S. Gourgou, C.J. O'Callaghan, C. Jouffroy-Zeller, P. Rat, D. Malka, F. Castan, J.-B. Bachet, FOLFIRINOX or gemcitabine as adjuvant therapy for pancreatic cancer, New Engl. J. Med. 379 (2018) 2395–2406, https://doi.org/10.1056/nejmoa1809775.
[7] K. Uesaka, N. Boku, A. Fukutomi, Y. Okamura, M. Konishi, I. Matsumoto, Y. Kaneoka, Y. Shimizu, S. Nakamori, H. Sakamoto, S. Morinaga, O. Kainuma, K. Imai, N. Sata, S. Hishinuma, H. Ojima, R. Yamaguchi, S. Hirano, T. Sudo, Y. Ohashi, Adjuvant chemotherapy of S-1 versus gemcitabine for resected pancreatic cancer: a phase 3, open-label, randomised, non-inferiority trial (JASPAC 01), Lancet 388 (2016) 248–257, https://doi.org/10.1016/S0140-6736(16)30583-9.
[8] D. Slade, PARP and PARG inhibitors in cancer treatment, Genes Dev. 34 (2020) 360–394, https://doi.org/10.1101/gad.334516.119.
[9] H. Zhu, M. Wei, J. Xu, J. Hua, C. Liang, Q. Meng, Y. Zhang, J. Liu, B. Zhang, X. Yu, S. Shi, PARP inhibitors in pancreatic cancer: Molecular mechanisms and clinical applications, Mol. Cancer 19 (2020) 1–15, https://doi.org/10.1186/s12943-020-01167-9.
[10] F. Xu, Y. Sun, S.Z. Yang, T. Zhou, N. Jhala, J. McDonald, Y. Chen, Cytoplasmic PARP-1 promotes pancreatic cancer tumorigenesis and resistance, Int J. Cancer 145 (2019) 474–483, https://doi.org/10.1002/ijc.32108.
[11] L.A. Byers, J. Wang, M.B. Nilsson, J. Fujimoto, P. Saintigny, J. Yordy, U. Giri, M. Peyton, Y.H. Fan, L. Diao, F. Masrorpour, L. Shen, W. Liu, B. Duchemann, P. Tumula, V. Bhardwaj, J. Welsh, S. Weber, B.S. Glisson, N. Kalhor, I.I. Wistuba, L. Girard, S.M. Lippman, G.B. Mills, K.R. Coombes, J.N. Weinstein, J.D. Minna, J. V. Heymach, Proteomic profiling identifies dysregulated pathways in small cell lung cancer and novel therapeutic targets including PARP1, Cancer Discov. 2 (2012) 798–811, https://doi.org/10.1158/2159-8290.CD-12-0112.
[12] A. Patsouris, K. Diop, O. Tredan, D. Nenciu, A. Gonçalves, M. Arnedos, M.-P. Sablin, P. Jézéquel, M. Jimenez, N. Droin, I. Bièche, C. Callens, A. Loehr, C. Vicier, C. Guerin, T. Filleron, F. André, Rucaparib in patients presenting a metastatic breast cancer with homologous recombination deficiency, without germline BRCA1/2 mutation, Eur. J. Cancer 159 (2021) 283–295, https://doi.org/10.1016/j.ejca.2021.09.028.
[13] E. Sachdev, R. Tabatabai, V. Roy, B.J. Rimel, M.M. Mita, PARP inhibition in cancer: an update on clinical development, Target Oncol. 14 (2019) 657–679, https://doi.org/10.1007/s11523-019-00680-2.
[14] M. Rose, J.T. Burgess, K. O'Byrne, D.J. Richard, E. Bolderson, PARP inhibitors: clinical relevance, mechanisms of action and tumor resistance, Front. Cell Dev. Biol. 8 (2020), 564601, https://doi.org/10.3389/fcell.2020.564601.
[15] J. Chi, S.Y. Chung, R. Parakrama, F. Fayyaz, J. Jose, M.W. Saif, The role of PARP inhibitors in BRCA mutated pancreatic cancer, Ther. Adv. Gastroenterol. 14 (2021), https://doi.org/10.1177/17562848211014818, 17562848211014818.
[16] L. Montemorano, D.S. Michelle, L.K. Bixel, Role of olaparib as maintenance treatment for ovarian cancer: the evidence to date, Onco Targets Ther. 12 (2019) 11497–11506, https://doi.org/10.2147/OTT.S195552.
[17] A.N.J. Tutt, J.E. Garber, B. Kaufman, G. Viale, D. Fumagalli, P. Rastogi, R. D. Gelber, E. de Azambuja, A. Fielding, J. Balmaña, S.M. Domchek, K.A. Gelmon, S. J. Hollingsworth, L.A. Korde, B. Linderholm, H. Bandos, E. Senkus, J.M. Suga, Z. Shao, A.W. Pippas, Z. Nowecki, T. Huzarski, P.A. Ganz, P.C. Lucas, N. Baker, S. Loibl, R. McConnell, M. Piccart, R. Schmutzler, G.G. Steger, J.P. Costantino, A. Arahmani, N. Wolmark, E. McFadden, V. Karantza, S.R. Lakhani, G. Yothers, C. Campbell, C.E. Geyer, Adjuvant Olaparib for Patients with BRCA1 - or BRCA2 -mutated breast cancer, New Engl. J. Med. 384 (2021) 2394–2405, https://doi.org/10.1056/nejmoa2105215.
[18] Y. Bi, I.I. Verginadis, S. Dey, L. Lin, L. Guo, Y. Zheng, C. Koumenis, Radiosensitization by the PARP inhibitor olaparib in BRCA1-proficient and deficient high-grade serous ovarian carcinomas, Gynecol. Oncol. 150 (2018) 534–544, https://doi.org/10.1016/j.ygyno.2018.07.002.
[19] J.M. Senra, B.A. Telfer, K.E. Cherry, C.M. McCrudden, D.G. Hirst, M.J. O'Connor, S. R. Wedge, I.J. Stratford, Inhibition of PARP-1 by olaparib (AZD2281) increases the radiosensitivity of a lung tumor xenograft, Mol. Cancer Ther. 10 (2011) 1949–1958, https://doi.org/10.1158/1535-7163.MCT-11-0278.
[20] S. Boussios, C. Abson, M. Moschetta, E. Rassy, A. Karathanasi, T. Bhat, F. Ghumman, M. Sheriff, N. Pavlidis, Poly (ADP-Ribose) Polymerase inhibitors: talazoparib in ovarian cancer and beyond, Drugs R D 20 (2020) 55–73, https://doi.org/10.1007/s40268-020-00301-8.
[21] S. Bogliolo, C. Cassani, M. Dominoni, V. Musacchi, P.L. Venturini, A. Spinillo, S. Ferrero, B. Gardella, Veliparib for the treatment of ovarian cancer, Expert Opin. Invest. Drugs 25 (2016) 367–374, https://doi.org/10.1517/13543784.2016.1146677.
[22] K.E. McCann, S.A. Hurvitz, Advances in the use of PARP inhibitor therapy for breast cancer, Drugs Context 7 (2018), 212540, https://doi.org/10.7573/dic.212540.
[23] D. Harrision, P. Gravells, R. Thompson, H.E. Bryant, Poly(ADP-Ribose) glycohydrolase (PARG) vs. Poly(ADP-Ribose) Polymerase (PARP) – function in genome maintenance and relevance of inhibitors for anti-cancer therapy, Front Mol. Biosci. 7 (2020) 191, https://doi.org/10.3389/fmolb.2020.00191.
[24] F. Quiñonero, C. Mesas, K. Doello, L. Cabeza, G. Perazzoli, C. Jimenez-Luna, A. R. Rama, C. Melguizo, J. Prados, The challenge of drug resistance in pancreatic ductal adenocarcinoma: a current overview, Cancer Biol. Med. 16 (2019) 688–699, https://doi.org/10.20892/j.issn.2095-3941.2019.0252.
[25] J. Bajaj, E. Diaz, T. Reya, Stem cells in cancer initiation and progression, J. Cell Biol. 219 (2020), e201911053, https://doi.org/10.1083/jcb.201911053.
[26] M. Gilabert, S. Launay, C. Ginestier, F. Bertucci, S. Audebert, M. Pophillat, Y. Toiron, E. Baudelet, P. Finetti, T. Noguchi, H. Sobol, D. Birnbaum, J.P. Borg, E. Charafe-Jauffret, A. Gonçalves, Poly(ADP-Ribose) polymerase 1 (PARP1) overexpression in human breast cancer stem cells and resistance to olaparib, PLoS One 9 (2014), e104302, https://doi.org/10.1371/journal.pone.0104302.
[27] A. Jarrar, F. Lotti, J. DeVecchio, S. Ferrandon, G. Gantt, A. Mace, G. Karagkounis, M. Orloff, M. Venere, M. Hitomi, J. Lathia, J.N. Rich, M.F. Kalady, Poly(ADP-Ribose) polymerase inhibition sensitizes colorectal cancer-initiating cells to chemotherapy, Stem Cells 37 (2019) 42–53, https://doi.org/10.1002/STEM.2929.
[28] F. Quiñonero, A. Cepero, D. Urbano, J.A. Muñoz-Gámez, S.M. Martín-Guerrero, D. Martín-Oliva, J. Prados, C. Melguizo, R. Ortiz, Identification of PARP-1 in cancer stem cells of gastrointestinal cancers: a preliminary study, J. Biosci. 46 (2021) 6, https://doi.org/10.1007/s12038-020-00135-1.
[29] K. Doello, C. Mesas, F. Quiñonero, G. Perazzoli, L. Cabeza, J. Prados, C. Melguizo, R. Ortiz, The antitumor activity of sodium selenite alone and in combination with gemcitabine in pancreatic cancer: an in vitro and in vivo study, Cancers 13 (2021) 3169, https://doi.org/10.3390/cancers13133169.
[30] A. Grada, M. Otero-Vinas, F. Prieto-Castrillo, Z. Obagi, V. Falanga, Research techniques made simple: analysis of collective cell migration using the wound healing assay, J. Invest. Dermatol. 137 (2017) e11–e16, https://doi.org/10.1016/J.JID.2016.11.020.
[31] B. García-Pinel, C. Porras-Alcalá, L. Cabeza, R. Ortiz, J. Prados, C. Melguizo, I. Cheng-Sánchez, J.M. López-Romero, F. Sarabia, Bengamide analogues show a potent antitumor activity against colon cancer cells: a preliminary study, Mar. Drugs 18 (2020) 240, https://doi.org/10.3390/md18050240.
[32] Y. Jiang, J. Martin, M. Alkadhimi, K. Shigemori, P. Kinchesh, S. Gilchrist, V. Kersemans, S. Smart, J.M. Thompson, M.A. Hill, M.J. O'Connor, B.R. Davies, A. J. Ryan, Olaparib increases the therapeutic index of hemithoracic irradiation compared with hemithoracic irradiation alone in a mouse lung cancer model, Br. J. Cancer 124 (2021) 1809–1819, https://doi.org/10.1038/s41416-021-01296-y.
[33] A. Sharma, K. Singh, A. Almasan, Histone H2AX phosphorylation: a marker for DNA damage, Methods Mol. Biol. 920 (2012) 613–626, https://doi.org/10.1007/978-1-61779-998-3_40.
[34] R.L. Siegel, K.D. Miller, A. Jemal, Cancer statistics, 2019, CA Cancer J. Clin. 69 (2019) 7–34, https://doi.org/10.3322/caac.21551.
[35] N. Khalaf, H.B. El-Serag, H.R. Abrams, A.P. Thrift, Burden of pancreatic cancer: from epidemiology to practice, Clin. Gastroenterol. Hepatol. 19 (2021) 876–884, https://doi.org/10.1016/j.cgh.2020.02.054.
[36] P. Hammel, C. Zhang, J. Matile, E. Colle, I. Hadj-Naceur, M.P. Gagaille, M. Bouattour, J. Cros, L. de Mestier, M. Lamuraglia, PARP inhibition in treatment of pancreatic cancer, Expert Rev. Anticancer Ther. 20 (2020) 939–945, https://doi.org/10.1080/14737140.2020.1820330.
[37] M.P. Dias, S.C. Moser, S. Ganesan, J. Jonkers, Understanding and overcoming resistance to PARP inhibitors in cancer therapy, Nat. Rev. Clin. Oncol. 18 (2021) 773–791, https://doi.org/10.1038/s41571-021-00532-x.
[38] R.L. Mintz, Y.H. Lao, C.W. Chi, S. He, M. Li, C.H. Quek, D. Shao, B. Chen, J. Han, S. Wang, K.W. Leong, CRISPR/Cas9-mediated mutagenesis to validate the synergy between PARP1 inhibition and chemotherapy in BRCA1-mutated breast cancer cells, Bioeng. Transl. Med. 5 (2020), e10152, https://doi.org/10.1002/btm2.10152.
[39] Y. Jiang, H. Dai, Y. Li, J. Yin, S. Guo, S.Y. Lin, D.J. McGrail, PARP inhibitors synergize with gemcitabine by potentiating DNA damage in non-small-cell lung cancer, Int. J. Cancer 144 (2019) 1092–1103, https://doi.org/10.1002/ijc.31770.
[40] Q. Wang, J. Xiong, D. Qiu, X. Zhao, D. Yan, W. Xu, Z. Wang, Q. Chen, S. Panday, A. Li, S. Wang, J. Zhou, Inhibition of PARP1 activity enhances chemotherapeutic efficiency in cisplatin-resistant gastric cancer cells, Int. J. Biochem. Cell Biol. 92 (2017) 164–172, https://doi.org/10.1016/j.biocel.2017.08.001.
[41] N.A. Yusoh, H. Ahmad, M.R. Gill, Combining PARP inhibition with platinum, ruthenium or gold complexes for cancer therapy, ChemMedChem 15 (2020) 2121–2135, https://doi.org/10.1002/cmdc.202000391.
[42] Y. Wang, Y. Kuramitsu, K. Tokuda, B. Baron, T. Kitagawa, J. Akada, S.I. Maehara, Y. Maehara, K. Nakamura, Gemcitabine induces poly (ADP-Ribose) polymerase-1 (PARP-1) degradation through autophagy in pancreatic cancer, PLoS One 9 (2014), e109076, https://doi.org/10.1371/journal.pone.0109076.
[43] D. Martin-Oliva, R. Aguilar-Quesada, F. O'Valle, J.A. Muñoz-Gámez, R. Martínez-Romero, R. García Del Moral, J.M. Ruiz De Almodóvar, R. Villuendas, M.A. Piris, F. J. Oliver, Inhibition of poly(ADP-ribose) polymerase modulates tumor-related gene expression, including hypoxia-inducible factor-1 activation, during skin carcinogenesis, Cancer Res. 66 (2006) 5744–5756, https://doi.org/10.1158/0008-5472.CAN-05-3050.
[44] L. Adesso, S. Calabretta, F. Barbagallo, G. Capurso, E. Pilozzi, R. Geremia, G. Delle Fave, C. Sette, Gemcitabine triggers a pro-survival response in pancreatic cancer

cells through activation of the MNK2/eIF4E pathway, Oncogene 32 (2013) 2848–2857, https://doi.org/10.1038/onc.2012.306.
[45] B.K. Samulitis, K.W. Pond, E. Pond, A.E. Cress, H. Patel, L. Wisner, C. Patel, R. T. Dorr, T.H. Landowski, Gemcitabine resistant pancreatic cancer cell lines acquire an invasive phenotype with collateral hypersensitivity to histone deacetylase inhibitors, Cancer Biol. Ther. 16 (2015) 43–51, https://doi.org/10.4161/15384047.2014.986967.
[46] C.B. Prasad, S.B. Prasad, S.S. Yadav, L.K. Pandey, S. Singh, S. Pradhan, G. Narayan, Olaparib modulates DNA repair efficiency, sensitizes cervical cancer cells to cisplatin and exhibits anti-metastatic property, Sci. Rep. 7 (2017) 1–15, https://doi.org/10.1038/s41598-017-13232-3.
[47] D. Wang, M. Wang, N. Jiang, Y. Zhang, X. Bian, X. Wang, T.M. Roberts, J.J. Zhao, P. Liu, H. Cheng, Effective use of PI3K inhibitor BKM120 and PARP inhibitor Olaparib to treat PIK3CA mutant ovarian cancer, Oncotarget 7 (2016) 13153–13166, https://doi.org/10.18632/oncotarget.7549.
[48] X. Mao, S. Du, Z. Yang, L. Zhang, X. Peng, N. Jiang, H. Zhou, Inhibitors of PARP-1 exert inhibitory effects on the biological characteristics of hepatocellular carcinoma cells in vitro, Mol. Med. Rep. 16 (2017) 208, https://doi.org/10.3892/MMR.2017.6568.
[49] X. Yang, C. Ndawula, X. Gong, J. Jin, JF-305, a pancreatic cancer cell line is highly sensitive to the PARP inhibitor olaparib, Oncol. Lett. 9 (2015) 757–761, https://doi.org/10.3892/ol.2014.2762.
[50] X. Lin, D. Chen, C. Zhang, X. Zhang, Z. Li, B. Dong, J. Gao, L. Shen, Augmented antitumor activity by olaparib plus AZD1775 in gastric cancer through disrupting DNA damage repair pathways and DNA damage checkpoint, J. Exp. Clin. Cancer Res. 37 (2018) 129, https://doi.org/10.1186/s13046-018-0790-7.
[51] Y. Lai, Z. Kong, T. Zeng, S. Xu, X. Duan, S. Li, C. Cai, Z. Zhao, W. Wu, PARP1-siRNA suppresses human prostate cancer cell growth and progression, Oncol. Rep. 39 (2018) 1901–1909, https://doi.org/10.3892/or.2018.6238.
[52] M.S. Goldberg, D. Xing, Y. Ren, S. Orsulic, S.N. Bhatia, P.A. Sharp, Nanoparticle-mediated delivery of siRNA targeting Parp1 extends survival of mice bearing tumors derived from Brca1-deficient ovarian cancer cells, Proc. Natl. Acad. Sci. USA 108 (2011) 745–750, https://doi.org/10.1073/pnas.1016538108.
[53] W. Waissi, A. Nicol, M. Jung, M. Rousseau, D. Jarnet, G. Noel, H. Burckel, Radiosensitizing pancreatic cancer with parp inhibitor and gemcitabine: an in vivo and a whole-transcriptome analysis after proton or photon irradiation, Cancers 13 (2021) 1–14, https://doi.org/10.3390/cancers13030527.